THERMAL EXPANSION MEASUREMENT OF COMPOSITE STRUCTURES

Matthew Norris and Darrell Oakes
Precision Measurements & Instruments, Inc.
Philomath, OR 97370

Ernest G. Wolff
Department of Mechanical Engineering
Oregon State University
Corvallis, OR 97331

ABSTRACT

Coefficients of thermal expansion (CTE) exceeding 0.5 ppm/K are routinely measured on small rod samples by quartz dilatometers. Special techniques based on Michelson interferometry are required to measure lower CTE's in the X-, Y, and Z-directions of complex structures such as plates, tubes, thin films and foils, honeycomb panels, unsymmetrical layups, low stiffness structures, and curved, bowed, twisted and/or tapered structures. Measurement of CTE values in the range 0 - +/-0.01 ppm/C over the range 25 - 1500K are discussed. Composite material parameters rather than optoelectronics considerations are emphasized. Edge, end, and thermal cycling effects are reviewed. Approaches to further improvements in accuracy are outlined.

KEY WORDS: Analysis/testing, Composites, Dimensional Stability

1. INTRODUCTION

Near-zero thermal expansion coefficients (CTE) are of interest to metrologists, materials scientists and structural materials engineers. This is because a wide variety of composite materials, ceramics and Invar type alloys require characterization and certification for many dimensionally stable components and structures. Current trends in nanotechnology, optomechanics, metrology, solid state devices and especially near-zero CTE composite materials require reliable CTE measurements with a resolution and accuracy of better than 10-7/K (1,2). Modulus-CTE relationships in crystalline fibers and studies of the magnitude and mechanism of residual stress relief (3-5) also require precise CTE measurements.

dimensions and low moisture absorbing resin matrices require qualification in terms of CTE (and CME) measurements. A wide variety of shapes and sizes are of interest, from individual fibers, tows, weaves and cloths, thin foils, plates, honeycomb sandwich panels, tubes (including tapered and curved antenna ribs), joints, end fittings, coated samples and actual components. The expansion characteristics are of interest in several directions as a function not only of temperature, but also of thermomechanical treatment, (especially thermal cycling), moisture content, attachments and constraints.

The optimum CTE measurement technique depends on the material/structure, temperature range and accuracy combination required. For example, LVDTs (linear variable differential transducers) together with quartz rods can give access to points on a large structure (6), but corrections are needed for the quartz expansion, misalignments and temperature effects on the LVDTs. Resolution of < 0.1 micron requires interferometry and Michelson interferometry is the most versatile approach toaccurate displacement measurement of objects of arbitrary size and shape (7-9). Since surfaces, edges, ends and residual stresses affect the CTE measured, one should not adjust the sample dimensions to fit measuring systems, as is required with Fizeau or Fabry-Perot interferometers. Some of our recent test results have been reported by others (2, 10-12). This paper reviews techniques, typical results and further improvements in CTE measurements.

2. THEORETICAL CONSIDERATIONS

2.1 Sample Bending/Twist. Composite material panels are frequently bowed and/or twisted due to fabrication procedures. Asymmetry may be caused by extra resin or ply layers, glue lines, ply orientations, variation in ply thicknesses and defects, such as in-plane delaminations. Heating or cooling initiates or magnifies bowing or twisting - normals to the sample surface (mirrors) will not remain parallel during a test and errors arise in the interferometer data.

2.2 Thick and/or stiff samples. Sample bowing can be monitored by an optical lever system; the angle of interferometer return beam divergence relates to the curvature variation with temperature. Photodetector signals record AC signals (fringe motion) which give in-plane strain; while the amplitude (DC level) records beam divergence caused by plate bowing. Correction of in-plane derived strain from changing amplitudes is complex as precise geometry of the optics and gain of the photodetector electronics play a part.

2.3 Thin and/or low stiffness samples. A weight can be placed on the sample to keep it flat. This allows accurate interferometer data to be taken but raises the question of the effect of such weight on the desired in-plane CTE values. We can use laminate theory to estimate the possible error on the reported CTE. To illustrate this approach, let us consider a sample plate 15.2 x 1.27 x 0.01 cm (with 8 plies each 0.0127 cm thick, for a CTE measured in the 15.2 cm direction. Suppose the plate is initially bowed so that the center sits 0.25 cm above the ends. We consider a minimum weight to flatten the sample. This then imposes a negative axial moment resultant. From standard mechanics we note that the center deflection,

$$d = P L^3/(48 E_f I) = 0.254 \text{ cm}$$

where $I = bh^3/12$ = moment of inertia of plate. With b = 1.27 cm, h = 0.01 cm, the

required load P (kg) will be 3.82e-7 E_f, where E_f is the flexural stiffness (kg/cm^2) dependent on the ply layup. The corresponding moment (applied at both ends) caused by this weight is PL/6 and the moment per unit width, is M/b, so that $\{M\} = M_x = -7.646e\text{-}7\ E_f$ (kg).

If we assume a $[0/+45/-45/90]_s$ layup of T300/5208 composite material, the flexural stiffness is 1.19e6 kg/cm^2 (16.94e6 psi) (13). This means a 0.45 kg (1.0 lb) load at center or a -0.9 kg moment resultant applied at both ends will exactly flatten this laminate. This moment will not induce a midplane strain, but rather curvatures k_1 of -0.009 (which serves to flatten the sample), k_2 of +0.005 strain/cm and twist of k_6 = 0.0034. A 1°c temperature change causes an average midplane strain of 0.8482e-6 cm/cm, the same as the calculated laminate CTE would predict. The average inplane strain does not change by more than 0.1% until the bending moment increases by over 1000X, a situation which will involve laminate damage. However, this assumes we are measuring the average strain across the sample cross section. In practice, our mirrors are set on the top surface. We can compare the surface strain due to a thermal load with and without the applied bending moment. This leads to the same conclusion: there is < 0.1% change in measured thermal strain when measuring only surface strain with applied bending moments. Typical results are given in section 4.3.

2.4 Asymmetrical Layups. With asymmetrical layups, the [B] stiffness matrix terms, or bending-extensional coupling terms, are non-zero, and an applied moment to flatten the sample will give erroneous CTE data. We can compare a $[0/60/-60]_T$ layup with and without a -0.9 kg moment per unit width. The axial CTE is 6.1e-6/C; with no moment, a 55 degree cooling will produce a midplane strain of -338.7 microstrain. With the moment, however, we would measure a midplane strain of -6043 microstrain. The exact error should be estimated with laminate theory for each (non-symmetrical) layup case. (An exception might be a class of laminates called Hygrothermally Curvature Stable Coupling (HTCC) laminates (14).

2.5 Microcracking. A weight may cause ply microcracking due to the resultant stresses. Again taking T300/5208 with the quasi-isotropic layup and a 0.9 kg applied M_1, the maximum stresses occur in the outer plies to a maximum level of about 1.24 MPa. This gives a first ply failure safety margin, R-value (13), of about 32. We conclude, therefore, that adding a weight to flatten a curved or twisted sample has a negligible (< 0.01%) effect on the measured CTE.

3. EXPERIMENTAL TECHNIQUES

3.1 Linear CTE Measurements. The most common CTE measurement required is on a thin plate, such as a 4 - 20 ply laminate coupon, generally with a quasi-isotropic ply layup. However, to characterize the fiber - matrix system, 0-deg and 90 degree unidirectional data are needed as well. In the past few years, requirements have expanded to through-thickness data, and for thick honeycomb panels, the effect of the adhesive layers and the behavior of the two face sheets separately. The presence of a honeycomb core introduces a macrostructure effect so that sample size becomes important. Moisture effects must be eliminated and the internal stress relief afforded by thermal cycling must be determined.

There are a variety of ways in which Michelson interferometers can be used. Figure 1 illustrates a horizontal approach while Figure 2 shows a vertical perspective.

gravity loading small (Zerodur or ULE glass) mirrors, polishing the ends or contacting the sample via points or lines with a mirror support system. Polished end faces need optical quality surfaces; flat, parallel and perpendicular to the end faces. When end/edge effects are minor, the double Michelson technique is best for solid rods and thick, solid plates since it allows the effective measuring beam to pass through the sample axis. Similarly, spring loaded mirrors work well for axial CTEs of tubes. However, the ends must be polished and the optical system is relatively complex.

3.2 Edge/end Effects. A composite sample near its edge will have different thermomechanical properties than within its bulk (15). The edge region size is similar to characteristic macrostructure, such as ply thicknesses or honeycomb cell widths, which commonly reach 0.65 cm. A 2.5 cm wide sample may easily be 50% edge material, and to the extent that the core affects the sandwich CTE there will be a 50% effect on the sandwich CTE. Such effects are minimized by using larger samples or by glueing of mirrors a distance in from the ends. However, even with a relatively low expansion, high vaccuum adhesive such as Varian TORR-SEAL, this leaves open the possibility of temperature induced mirror rotation due to the glue line. We have experimented with two new methods to avoid end effects: The first is called the pin method (Figure 3). Here a tungsten wire pin is spring loaded against a small hole drilled in the sample surface. This places a slight compression load onto the sample and does not always reflect the exact sample dimensions when there is a directional change, such as transition from cooling to heating.

The blade method (Figure 4) employs a shallow, 0.3 mm wide groove inscribed on the sample perpendicular to the measurement direction. A reflecting steel razor blade is connected to 75 mm long quartz rod. A ULE mirror may also be attached to the blade. Razor tilt response during sample bending is adjusted by the length of the quartz rod. This system assures that there is instantaneous response to direction changes.

3.3 Tube Structures. Figure 5 shows mirrors which are spring loaded to the ends of a tube sample so that laser beams can pass close to the tube axis. This minimizes errors due to tube bending but does include the sample ends. The razor method can be modified for tubes if end effects are suspected. Figure 6 shows modified bolts for support of reflecting surfaces at the centerline of struts with clevis fittings.

3.4 Low Stiffness Structures. Low stiffness structures present special measurement problems. Thin films or foils, fibers, tows, yarns, unreinforced fabrics and honeycomb structures without face sheets are typical examples. In-plane CTE of thin films are readily measured with Michelson interferometry if they can be treated as low stiffness thin plates, viz., by adding weights. Honeycombs can be measured along the cell directions (material direction) in the same way. Problems arise with short length thin films or with directions across the cells in a honeycomb. In these cases alternative methods to Michelson interferometry must be considered. Speckle interferometry is a good candidate for inplane film or fiber CTE, holographic interferometry may be considered for 3-D deformation of a honeycomb structure. However, resolution, complexity (and cost) may be drawbacks. We have recently measured the cell deformations of a honeycomb structure to a resolution of about 0.01 mm over the range -150 to +100C. This was done by optical magnification and imaging of selected points on the cell structure with a computerized video image system and special magnifying optics. Calibration is made by lightly supporting a thin strip of material

with known CTE on the surface of the honeycomb.

3.5 Expanded Temperature Range with Laser Interferometry. We have seen increased interest in CTE measurements to temperatures below liquid nitrogen (77K), at least to the region 10-50K. These are made with liquid helium in the coolers shown in Figures 1 and 2. Cryogenic coolers with moving parts tend to impose excessive vibration for interferometric measurements but are useful for thermal cycling in helium atmospheres. Narrow band pass filters for the reflected laser beams allow operation to over 1500 K. The thermocouples are read to +/- 0.1 K but their accuracy is rarely better than +/- 0.5K. Temperature capabilities for mirrors include aluminized ULE to about 700K, polished silicon wafers to 1100K and molybdenum to over 2000K.

3.6 Signal Processing. Signal processing for accurate fringe interpolation will not be discussed here; various schemes have been devised (7, 9, 16- 19). Software must deal with changes in beam divergence, fluctuations in signal amplitude, spikes from microcracking, and loss of signals due to excessive sample bending. We use both custom designed software and continuous chart recording for verification.

4. RESULTS

4.1 Out-of-Plane Motions. The effects of sample bend/twist are shown in Figure 7 for a 4.0 x 18.0 x 0.01 cm graphite fiber/resin composite specimen which was measured in the 18 cm direction three times. The blade method was used to connect the two reflective surfaces, whose separation constitutes the length change, to the sample. On the first two measurements there as no weight placed on the sample to keep it flat. One side faced up during the first measurement; the other during the second. With side #1 facing up, the total strain was 600 ppm greater than with side #1 facing down, giving CTEs of -0.71 ppm/C and -0.99 ppm/C, respectively. When 50 grams of mass was uniformly placed on side #1 the prior concave bending was eliminated and the CTE was correctly measured as -0.88 ppm/C, near the average of the other two measurements. (The variation in these three measurements is far greater than the repeatability and accuracy of these values (0.01 ppm/C).

4.2 Sides of Tubes. Figure 8 shows the variation in CTE of individualopposing sides of a tube structure compared to the CTE of the central axis of the tube. The T50/954-2A resin tube had a square cross section with rounded corners. The blade method used on the sides meant that the corner edges were included, and one side at 0.14 ppm/Ccontrasts with -0.03 ppm/C with the opposite side. The axial measurement (giving +0.02 ppm/C) used both complete end surfaces as described above, and clearly demonstrates the dangers in measuring only one side.

4.3 Struts and Larger Components. Figure 9 shows test results on a section of a tubular strut. Aluminum end fittings were added and gave the results shown in Figure 10 for the full 150 cm structure. The negative CTE tube added to the positive CTE fittings gave the expected uniform, near-zero CTE of +0.007 ppm/C. The slight hysteresis reflects the finite heating/cooling rates, although the net +0.5 microstrain after the two cycles indicates some internal sample adjustment, e.g., microcracking, common for adhesive joints after thermal cycling. The contact points where this low CTE strut can be realized must be identified and both the measurement and application must use identical contact points (See Figure 6).

axes of symmetry. Figure 11 gives results for a triaxial woven honeycomb panel. The through-thickness measurement was made with the vertical system of Figure 2. It is important here to cover a substantial area of the structure on both sides because typical point to point variations in expansion are on the same order of magnitude as the total expansion. The axial and transverse expansions were measured with the blade method on two samples which were 4.0 cm wide by 18.0 cm in the measurement direction. Measurement in both axial and transverse directions at the same time is necessary when determining the thermal expansion of a tube diameter, as often the cross section of a tube changes shape as it expands.

4.5 Ultralow CTE. Telescope and interferometer construction materials require further advances in CTE accuracy and resolution. Our laboratory was recently asked to verify an expected CTE of 10^{-9}/K of a ULE glass laser cavity standard for NASA's "Lasers in Space" program. The application was measurement of temporal characteristics of linewidth variations by examining beat note signals from two actively stabilized lasers both on earth and in space. This work is part of a broad requirement for dimensional stability in space programs. The ULE cylinder was Al-coated by CVD at the ends and measured via the double Michelson method. The optics were adjusted so that voltage signals from each interferometer were close to zero volts. This meant that the computerized DAQ system could read the amplified photodetector signals at the maximum resolution, namely five and 1/2 significant figures. The peak to peak signal of 2 volts then represented a 3164 angstrom length change, so that the total resolution was 1.58e-12 m. With a L_o of 4.9784 cm, this meant a strain sensitivity of 3.17e-11. Interferometer analog voltage/temperature data pairs were recorded each second. Computerized regression analysis fit to a polynomial curve is compared to a reference signal based on the entire system except for the sample. Figure 12 shows the instantaneous slope of the regression curve. The zero CTE point is seen to occur at about 3°C.

5. DISCUSSION

Measurement errors, sensitivity and noise estimates (7,16-20) suggest increased resolution and accuracy (to ppb/C) depend on further improvements in frequency stabilized lasers, drift compensation, noise suppression and AC fringe detection. High accuracy temperature measurement is also critical to ppb/K CTE measurement. Both absolute temperature and temperature gradients must be accurately controlled and characterized. The double self-compensating Michelson interferometer (7) uses a He-Ne laser whose absolute wavelength changes were 2.5 x10^{-3}nm/K (2 x 10^{3}MHz/K) with a drift of +/- 2.5% in 8 hours. This drift is an impediment because measurements over broad temperature ranges take several hours. One approach would be to make the interference beam paths differential and self compensating, e.g., through use of identical beam paths. The rms phase noise is on the order of10^{-3} for a 0.5 mW HeNe laser and a typical 4 MHz bandwidth, which corresponds to a resolution of about 0.3 nm. Misalignments must be reduced to a few nanoradians. One approach would be to incorporate an auxiliary interferometer whose output serves as a (piezoelectric transducer driven) feedback loop to keep the primary alignment tied to a zero or non-deviating null point position. Past work also indicates that spatial filtering and use of beam expanders improve accuracy on longer samples (>200cm).

6. CONCLUSIONS

Current techniques for general CTE measurements on arbitrary size or shape of composite material coupons, components and structures have been reviewed. While electro-optics techniques and improved data acquisition are pushing a level of accuracy of ppb/C, special considerations are still needed to account for material behavior. Both manufacturing quality (e.g., adhesive thickness) and design (e.g. layup) as well as sample size and shape affect the accuracy of the CTE measurement.

7. ACKNOWLEDGMENTS

PMIC gratefully acknowledges the assistance of Hong Chen and Antonia Wolff with analysis of interferometric data. OSU wishes to acknowledge the assistance of students Gwo-Sheng Peng, (signal processing), Eric Paterson, Morgan Talarczyk and Paul Sawyer (ULE glass), and Tyrus Monson and Alicia Fichter (video imaging of honeycomb structures). Thanks are also due to Alice Wolff for administrative support.

8. REFERENCES

1) D. Rapp, NASA Tech Brief 18 (9), JPL New Tech. Rept. NPO-18984 Sept (1994)
2) J.G. Hamilton and J.M. Patterson, Proceedings International Conference on Composite Materials ICCM/9 Madrid, Ed. A. Miravete, Woodhead Publ. Ltd., Proceedings Vol. VI, 108-119 (1993)
3) E.G. Wolff, B.K. Min and M.H. Kural J. Mat. Sci. 20, 1141-1149 (1985)
4) E.G. Wolff, W.H. Dittrich, R.C. Savedra and C. Sve, Composites 323-328 July (1982)
5) E.G. Wolff J. Composite Materials 21, 81-97 (1987)
6) A. Nanjyo, M. Mohri and T. Ishikawa 39th Intl. SAMPE Symp. 39, 541-550, April, (1994)
7) E.G. Wolff and R.C. Savedra, Rev. Sci.Instr. 56, 1313-1319 (1985)
8) H. Billing, K. Maischberger, A. Rudiger, R. Schilling, J. Schnupp and W. Winkler J. Phys. E: Sci. Instrum, 12, (1979).
9) G.S. Peng and E.G. Wolff, Thermochimica Acta 218, 101-112 (1993)
10) C. Blair and J. Zakrzewski 22nd Intl. SAMPE Tech. Conf. Boston, Nov 6-8, p918-931 (1990)
11) C. Blair and J. Zakrzewski 22nd Intl. SAMPE Tech. Conf. Boston, Nov 6-8, p932-942 (1990)
12) C. Blair and G.A. Jensen, 37th Intl. SAMPE Symposium 37, 115-127 (1992)
13) S.Tsai,"Composite Design" Think Composites, Dayton, Ohio
14) S.J. Winkler and S.C. Hill, Proceedings ICCM/VIII, Honolulu, Paper 2-I-3, July 15-19, (1991)
15) M.H. Kural and A.M. Ellison, SAMPE Journal p20-26 Sept/Oct (1980)
16) S.A. Eselun and E.G. Wolff, Instrument Society of America Transactions 19(1), 59-64 (1980)
17) S.A. Eselun, R.C. Savedra and E.G. Wolff Air Force Space Division Report SD-TR-81-113 18 December (1981)
18) G.S. Peng Ph.D. Thesis, Department of Mechanical Engineering, Oregon State University (1992)
19) E.G. Wolff and S. Eselun, Rev. Sci. Instr. 50, 502-506 (1979)

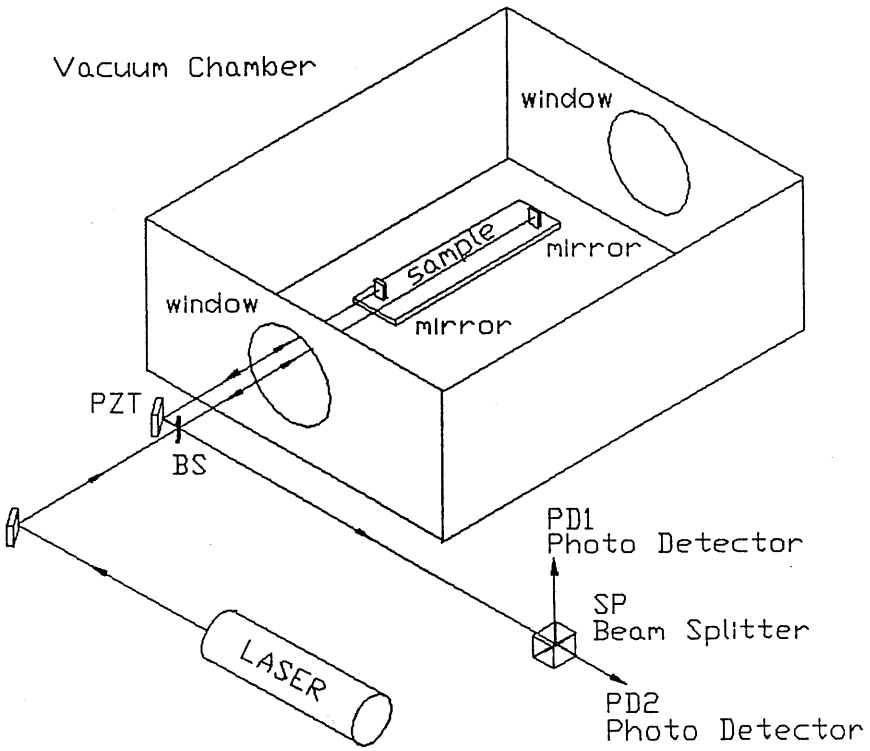

Figure 1. Horizontal LASER Interferometer

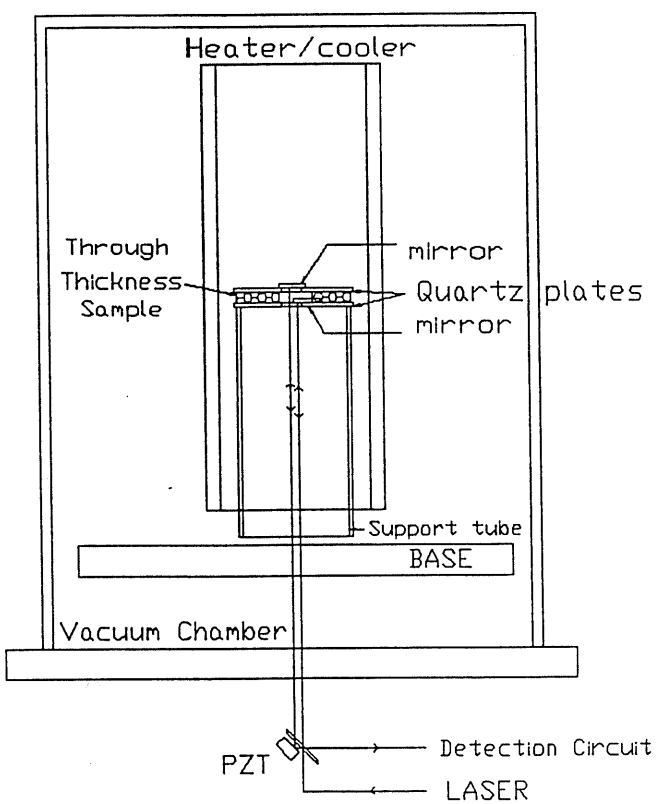

Figure 2. Vertical CTE System

Fig. 3 Pin System

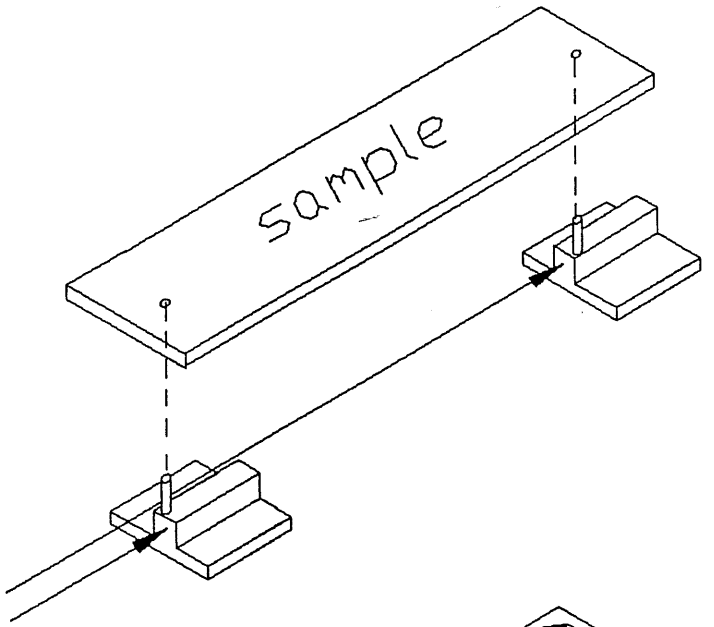

Fig. 4 Blade System

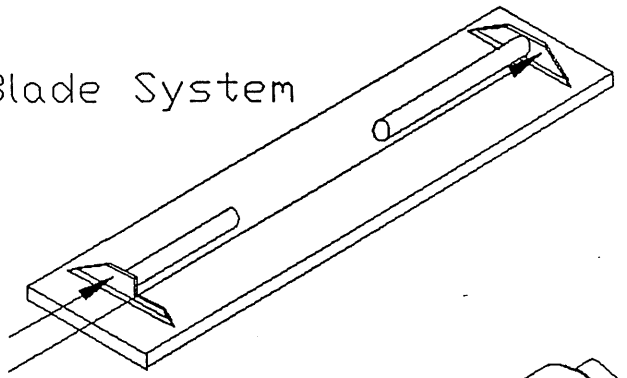

Fig. 5 Axial Tube System

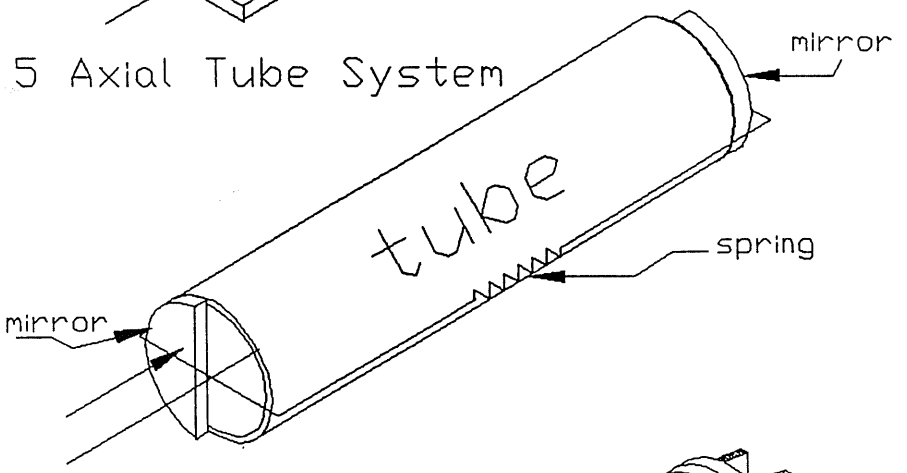

Fig. 6 Modified Clevis Bolt

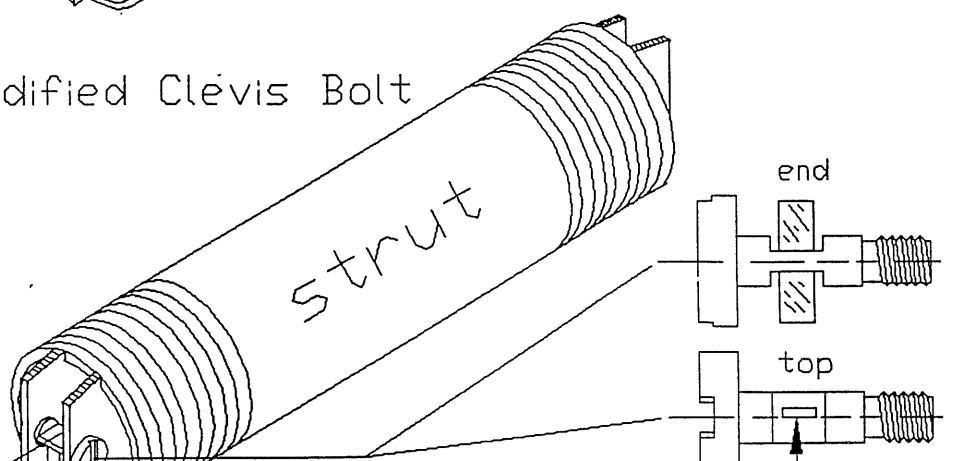

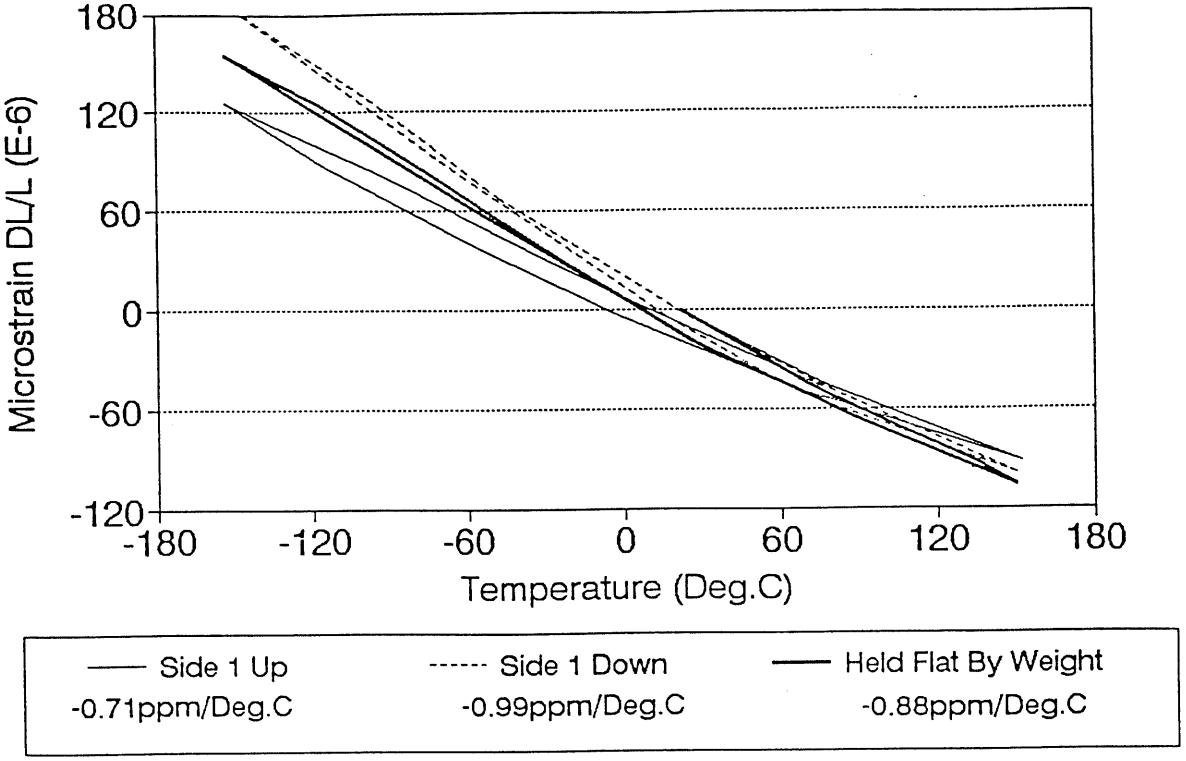

Figure 7. Thermal Expansion of Unidirectional Graphite/Resin Panel

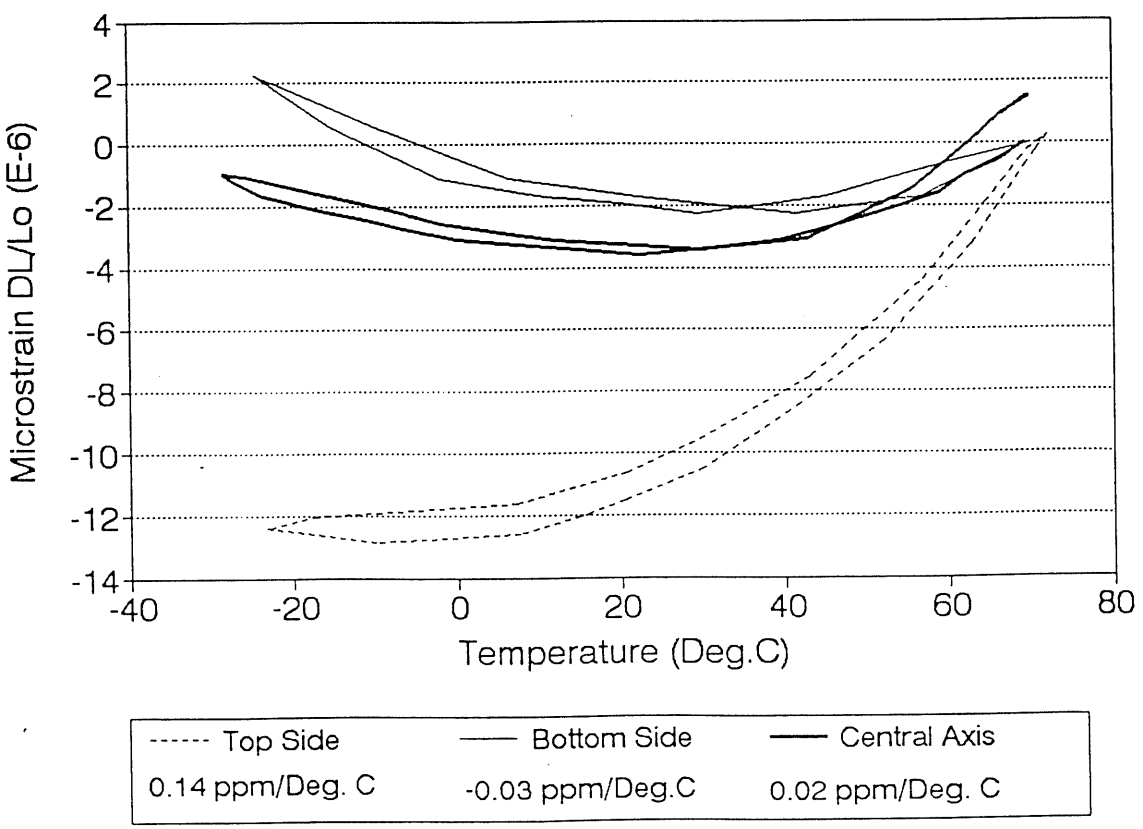

Figure 8. Thermal Expansion of T50/954-2A [0/63.5/0/-63.5]s Square Tube

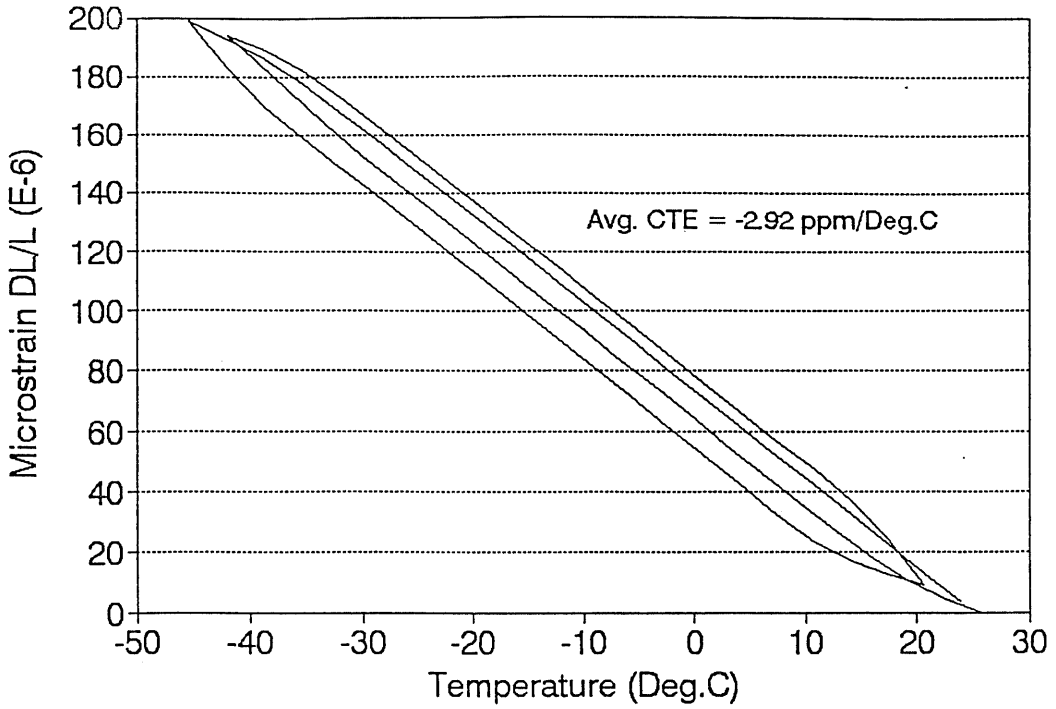

Figure 9. Thermal Expansion of 5cm DIA Graphite/Epoxy Tube

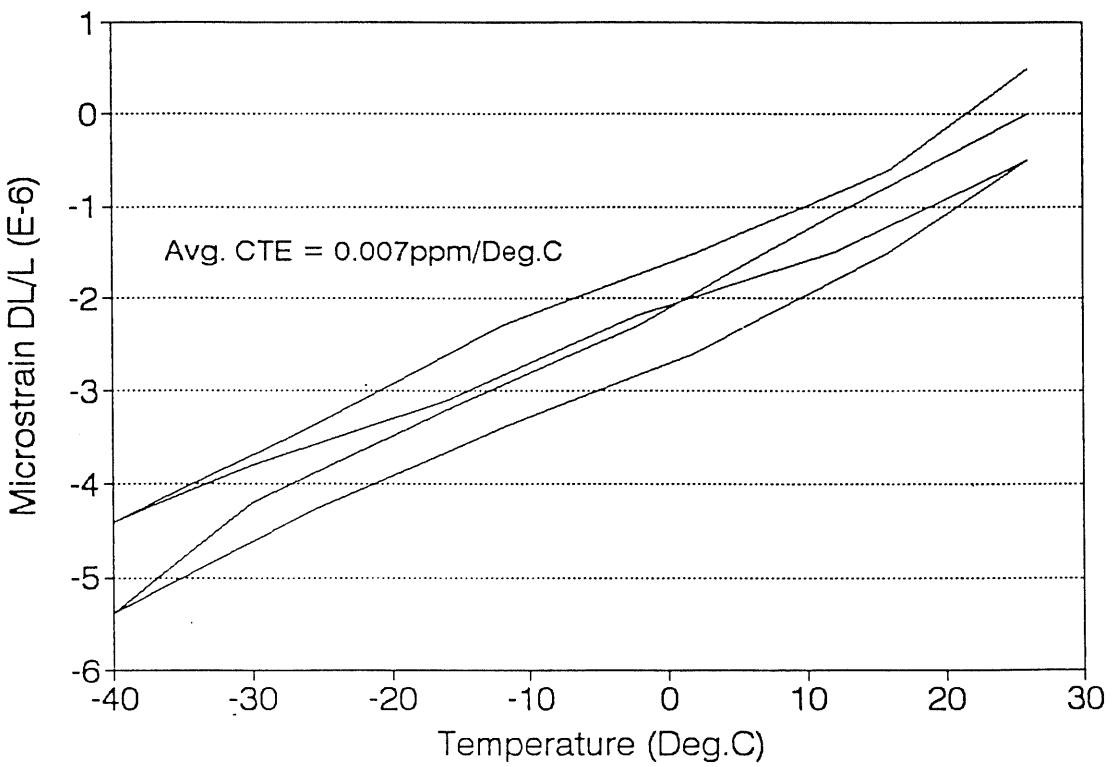

Figure 10. Thermal Expansion of 5 cm diameter Graphite/Epoxy Tube with Al End Fittings

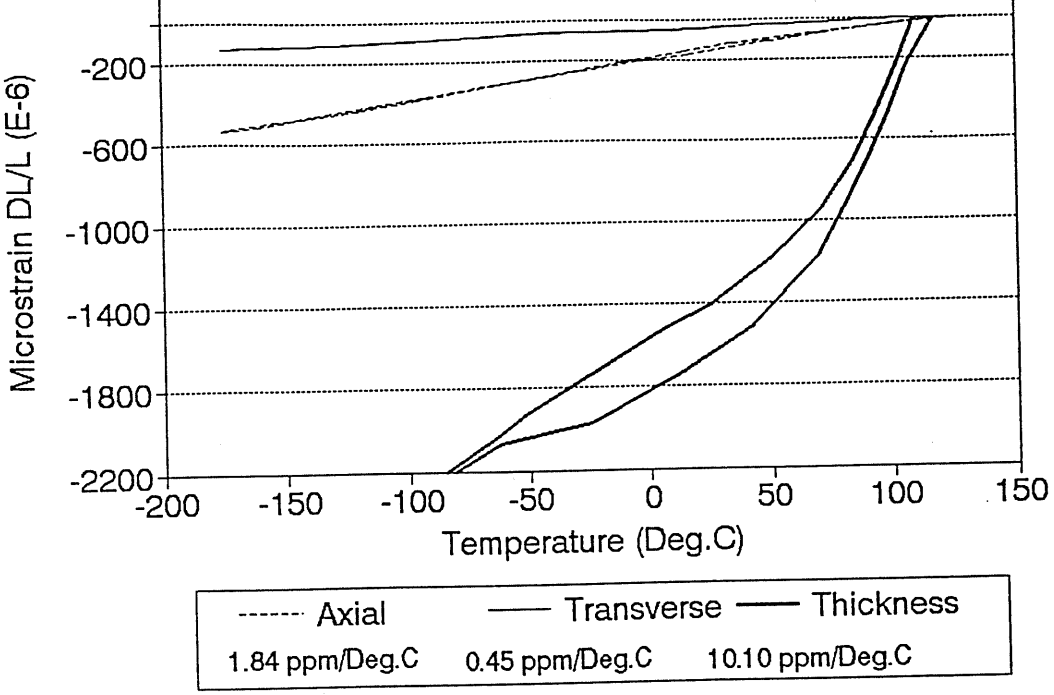

Figure 11. Thermal Expansion of Triax Woven, Honeycomb Panel

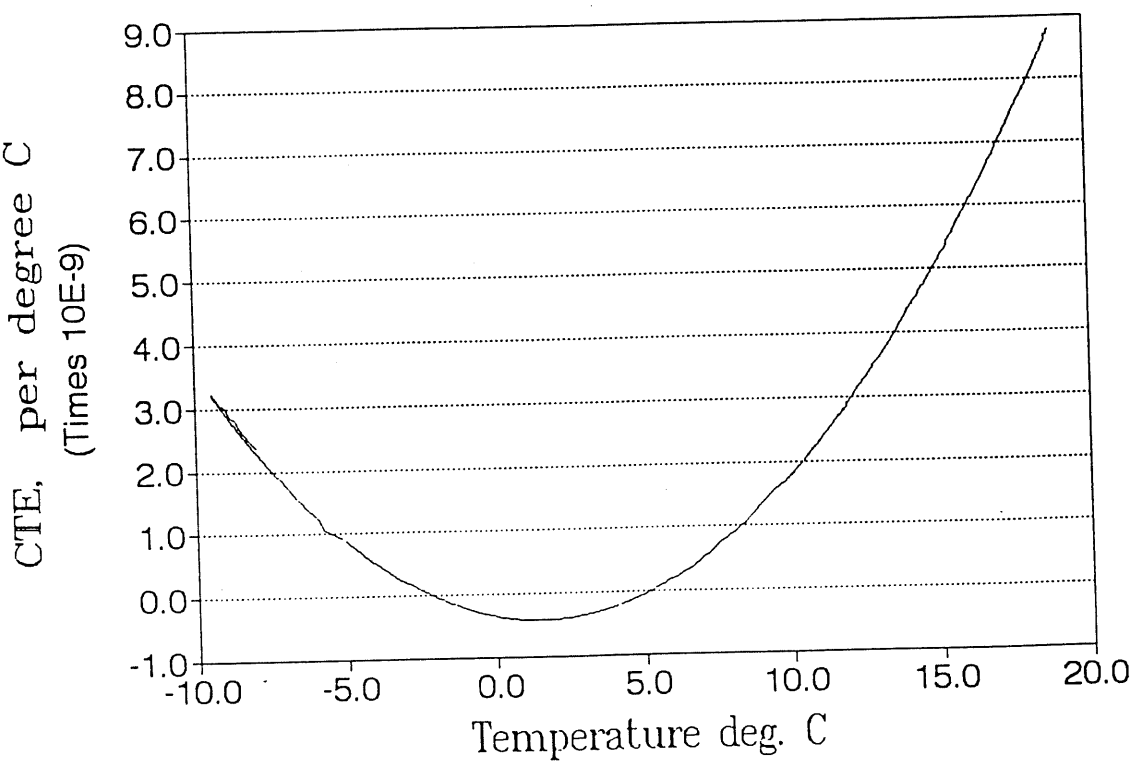

Figure 12. Instantaneous CTE of a ULE glass Tube